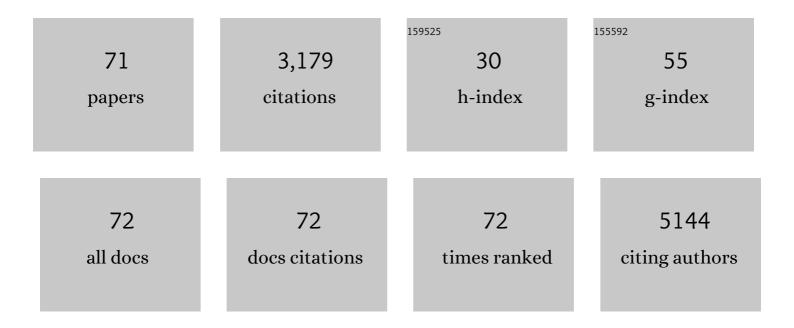
## Qiang Wang

List of Publications by Year in descending order

Source: https://exaly.com/author-pdf/9100220/publications.pdf Version: 2024-02-01



#	Article	IF	CITATIONS
1	Design of two-dimensional halide perovskite composites for optoelectronic applications and beyond. Materials Advances, 2022, 3, 756-778.	2.6	14
2	Defect Engineering of Ultrathin WO <sub>3</sub> Nanosheets: Implications for Nonlinear Optoelectronic Devices. ACS Applied Nano Materials, 2022, 5, 1169-1177.	2.4	15
3	Ultrafast Generation of Coherent Phonons in Two-Dimensional Bismuthene. Journal of Physical Chemistry Letters, 2022, 13, 3072-3078.	2.1	5
4	Carbon nano-onion encapsulated cobalt nanoparticles for oxygen reduction and lithium-ion batteries. Journal of Materials Chemistry A, 2021, 9, 7227-7237.	5.2	21
5	Rational synthesis of novel "giant―CuInTeSe/CdS core/shell quantum dots for optoelectronics. Nanoscale, 2021, 13, 15301-15310.	2.8	3
6	Unveiling the dimension-dependence of femtosecond nonlinear optical properties of tellurium nanostructures. Nanoscale Horizons, 2021, 6, 918-927.	4.1	12
7	In situ observation of the crystal structure transition of Pt–Sn intermetallic nanoparticles during deactivation and regeneration. Chemical Communications, 2021, 57, 5454-5457.	2.2	2
8	Two-Dimensional Bismuthene Showing Radiation-Tolerant Third-Order Optical Nonlinearities. ACS Applied Materials & Interfaces, 2021, 13, 21626-21634.	4.0	19
9	The Renascence of One Ancient Recipe for Synthesizing Luminescent Cs <sub>4</sub> PbBr <sub>6</sub> Microcrystals. Physica Status Solidi - Rapid Research Letters, 2021, 15, 2100169.	1.2	2
10	Boosting Cascade Electron Transfer for Highly Efficient CO <sub>2</sub> Photoreduction. Solar Rrl, 2021, 5, 2100558.	3.1	11
11	Understanding the Role of Oxygen and Hydrogen Defects in Modulating the Optoelectronic Properties of P-Type Metal Oxide Semiconductors. Chemistry of Materials, 2021, 33, 7829-7838.	3.2	12
12	Template-free synthesis of a yolk–shell Co <sub>3</sub> O <sub>4</sub> /nitrogen-doped carbon microstructure for excellent lithium ion storage. Journal of Materials Chemistry A, 2021, 9, 24548-24559.	5.2	18
13	Antimonene-based flexible photodetector. Nanoscale Horizons, 2020, 5, 124-130.	4.1	51
14	Tunable nonlinear optical responses and carrier dynamics of two-dimensional antimonene nanosheets. Nanoscale Horizons, 2020, 5, 1420-1429.	4.1	15
15	Manipulating the Optoelectronic Properties of Quasi-type II CuInS <sub>2</sub> /CdS Core/Shell Quantum Dots for Photoelectrochemical Cell Applications. ACS Applied Materials & Interfaces, 2020, 12, 36277-36286.	4.0	23
16	2D materials towards ultrafast photonic applications. Physical Chemistry Chemical Physics, 2020, 22, 22140-22156.	1.3	38
17	Fluorescence Lifetime-Tunable Water-Resistant Perovskite Quantum Dots for Multidimensional Encryption. ACS Applied Materials & amp; Interfaces, 2020, 12, 43073-43082.	4.0	30
18	Selective Photocatalytic Hydrogenation of α,β-Unsaturated Aldehydes on Au/CuCo <sub>2</sub> O <sub>4</sub> Nanotubes under Visible-Light Irradiation. ACS Sustainable Chemistry and Engineering, 2020, 8, 8288-8294.	3.2	21

QIANG WANG

#	Article	IF	CITATIONS
19	In Situ Growth of 3D/2D (CsPbBr <sub>3</sub> /CsPb <sub>2</sub> Br <sub>5</sub> ) Perovskite Heterojunctions toward Optoelectronic Devices. Journal of Physical Chemistry Letters, 2020, 11, 6007-6015.	2.1	54
20	Solution-phase vertical growth of aligned NiCo2O4 nanosheet arrays on Au nanosheets with weakened oxygen–hydrogen bonds for photocatalytic oxygen evolution. Nanoscale, 2020, 12, 6195-6203.	2.8	23
21	<i>In situ</i> growth of luminescent perovskite fibers in natural hollow templates. Chemical Communications, 2019, 55, 11056-11058.	2.2	6
22	Disentangling the Luminescent Mechanism of Cs <sub>4</sub> PbBr <sub>6</sub> Single Crystals from an Ultrafast Dynamics Perspective. Journal of Physical Chemistry Letters, 2019, 10, 6572-6577.	2.1	29
23	In Situ Integration of ReS <sub>2</sub> /Ni <sub>3</sub> S <sub>2</sub> p-n Heterostructure for Enhanced Photoelectrocatalytic Performance. ACS Applied Materials & Interfaces, 2019, 11, 40014-40021.	4.0	37
24	Confinement effect of natural hollow fibers enhances flexible supercapacitor electrode performance. Electrochimica Acta, 2018, 260, 204-211.	2.6	22
25	2D bismuthene fabricated <i>via</i> acid-intercalated exfoliation showing strong nonlinear near-infrared responses for mode-locking lasers. Nanoscale, 2018, 10, 21106-21115.	2.8	115
26	Construction of Au/CuO/Co <sub>3</sub> O <sub>4</sub> Tricomponent Heterojunction Nanotubes for Enhanced Photocatalytic Oxygen Evolution under Visible Light Irradiation. ACS Sustainable Chemistry and Engineering, 2018, 6, 8801-8808.	3.2	30
27	Negatively charged 2D black phosphorus for highly efficient covalent functionalization. Materials Chemistry Frontiers, 2018, 2, 1700-1706.	3.2	56
28	Solvent-Free Mechanosynthesis of Composition-Tunable Cesium Lead Halide Perovskite Quantum Dots. Journal of Physical Chemistry Letters, 2017, 8, 1610-1614.	2.1	173
29	Disentangling the Photocatalytic Hydrogen Evolution Mechanism of One Homogeneous Cobalt-Coordinated Polymer. Journal of Physical Chemistry C, 2016, 120, 28456-28462.	1.5	11
30	Preparation of large size, few-layer black phosphorus nanosheets via phytic acid-assisted liquid exfoliation. Chemical Communications, 2016, 52, 8107-8110.	2.2	86
31	Small molecule-assisted fabrication of black phosphorus quantum dots with a broadband nonlinear optical response. Nanoscale, 2016, 8, 15132-15136.	2.8	71
32	Iron-Doped Carbon Nitride-Type Polymers as Homogeneous Organocatalysts for Visible Light-Driven Hydrogen Evolution. ACS Applied Materials & Interfaces, 2016, 8, 617-624.	4.0	135
33	Developing carbon-nitride nanosheets for mode-locking ytterbium fiber lasers. Optics Letters, 2016, 41, 1221.	1.7	23
34	In situ preparation of a MOF-derived magnetic carbonaceous catalyst for visible-light-driven hydrogen evolution. RSC Advances, 2016, 6, 2011-2018.	1.7	35
35	Well-controlled layer-by-layer assembly of carbon dot/CdS heterojunctions for efficient visible-light-driven photocatalysis. Journal of Materials Chemistry A, 2015, 3, 16613-16620.	5.2	66
36	Controlled engineering of WS2 nanosheets–CdS nanoparticle heterojunction with enhanced photoelectrochemical activity. Solar Energy Materials and Solar Cells, 2015, 141, 260-269.	3.0	55

QIANG WANG

#	Article	IF	CITATIONS
37	Unexpected optical limiting properties from MoS <sub>2</sub> nanosheets modified by a semiconductive polymer. Chemical Communications, 2015, 51, 12262-12265.	2.2	60
38	Broadband optical limiting response of a graphene–PbS nanohybrid. Nanoscale, 2015, 7, 9268-9274.	2.8	61
39	Singlet fission induced giant optical limiting responses of pentacene derivatives. Materials Horizons, 2015, 2, 619-624.	6.4	29
40	Rational design of small indolic squaraine dyes with large two-photon absorption cross section. Chemical Science, 2015, 6, 761-769.	3.7	69
41	Size-Dependent Nonlinear Optical Properties of Atomically Thin Transition Metal Dichalcogenide Nanosheets. Small, 2015, 11, 694-701.	5.2	160
42	Oneâ€Pot Synthesis of Highly Luminescent Carbon Quantum Dots and Their Nontoxic Ingestion by Zebrafish for In Vivo Imaging. Chemistry - A European Journal, 2014, 20, 5640-5648.	1.7	74
43	Mitigation of metal-mediated losses by coating Au nanoparticles with dielectric layer in plasmonic solar cells. RSC Advances, 2013, 3, 16080.	1.7	21
44	Understanding the Unconventional Effects of Halogenation on the Luminescent Properties of Oligo(Phenylene Vinylene) Molecules. Chemistry - an Asian Journal, 2013, 8, 3091-3100.	1.7	27
45	K7[CollIColl(H2O)W11O39]: a molecular mixed-valence Keggin polyoxometalate catalyst of high stability and efficiency for visible light-driven water oxidation. Energy and Environmental Science, 2013, 6, 1170.	15.6	285
46	Improved synthesis of PbSxSe1â^'x ternary alloy nanocrystals and their nonlinear optical properties. New Journal of Chemistry, 2013, 37, 1692.	1.4	12
47	Graphene in Light: Design, Synthesis and Applications of Photoâ€active Graphene and Grapheneâ€Like Materials. Small, 2013, 9, 1266-1283.	5.2	129
48	Core–shell plasmonic nanostructures to fine-tune long ``Au nanoparticle-fluorophore'' distance and radiative dynamics. Colloids and Surfaces A: Physicochemical and Engineering Aspects, 2013, 421, 101-108.	2.3	27
49	A Facile Phosphineâ€Free Method for Synthesizing PbSe Nanocrystals with Strong Optical Limiting Effects. Chemistry - an Asian Journal, 2013, 8, 912-918.	1.7	15
50	Arsenic Precipitation in the Bioleaching of Realgar Using <i>Acidithiobacillus ferrooxidans</i> . Hindawi Journal of Chemistry, 2013, 2013, 1-5.	1.6	7
51	DFT Study on the Mechanism of PtCl <sub>2</sub> -Catalyzed Rearrangement of Cyclopropenes to Allenes. Organometallics, 2012, 31, 4020-4030.	1.1	13
52	Electrochemical properties of nanostructured cobalt hexacyanoferrate containing K+ and Cs+ synthesized in water-in-oil AOT reverse microemulsions. Journal of Electroanalytical Chemistry, 2012, 674, 30-37.	1.9	7
53	Surface alteration of realgar (As(4)S(4)) by Acidithiobacillus ferrooxidans. International Microbiology, 2012, 15, 9-15.	1.1	10
54	Distinct exciton migration pathways induced by steric hindrance in Langmuir–Blodgett films of two novel cruciform molecular wires. Chemical Physics Letters, 2011, 518, 65-69.	1.2	4

QIANG WANG

#	Article	IF	CITATIONS
55	Spectroscopic and molecular modeling evidence of clozapine binding to human serum albumin at subdomain IIA. Spectrochimica Acta - Part A: Molecular and Biomolecular Spectroscopy, 2011, 79, 1202-1209.	2.0	42
56	A Simple Method for the Synthesis of Fe-Co Prussian Blue Analogue with Novel Morphologies, Different Structures, and Dielectric Properties. Synthesis and Reactivity in Inorganic, Metal Organic, and Nano Metal Chemistry, 2011, 41, 1108-1113.	0.6	6
57	Magnetism study of CI xCoy[Fe(CN)6]·zH2O (CI=Rb,Cs) Prussian blue nanoparticles. Journal of the Iranian Chemical Society, 2010, 7, S123-S129.	1.2	5
58	Strong Twoâ€Photon Excited Fluorescence and Stimulated Emission from an Organic Single Crystal of an Oligo(Phenylene Vinylene). Angewandte Chemie - International Edition, 2010, 49, 732-735.	7.2	119
59	Structure and Photoinduced Electron Transfer in DNA Hairpin Conjugates Possessing a Tethered $5\hat{a}\in^2$ -Pyrenecarboxamide. Journal of Physical Chemistry B, 2009, 113, 16276-16284.	1.2	24
60	Dynamics of Photochemical Electron Injection and Efficiency of Electron Transport in DNA. Journal of the American Chemical Society, 2009, 131, 16790-16797.	6.6	37
61	Getting to guanine: mechanism and dynamics of charge separation and charge recombination in DNA revisited. Photochemical and Photobiological Sciences, 2008, 7, 534-539.	1.6	36
62	Photoinduced charge separation in pyrenedicarboxamide-linked DNA hairpins. Photochemical and Photobiological Sciences, 2008, 7, 1501.	1.6	13
63	Reversible Bridge-Mediated Excited-State Symmetry Breaking in Stilbene-Linked DNA Dumbbells. Journal of Physical Chemistry B, 2008, 112, 3838-3843.	1.2	33
64	Electronic energy delocalization and dissipation in single- and double-stranded DNA. Proceedings of the United States of America, 2007, 104, 4794-4797.	3.3	168
65	Molecular Wire Behavior in π-Stacked Donor-Bridge-Acceptor Tertiary Arylureas. Journal of the American Chemical Society, 2007, 129, 9848-9849.	6.6	45
66	Ultrafast Energy Delocalization and Electron Transfer Dynamics in 2-Aminopurine-Containing Trinucleotides. Photochemistry and Photobiology, 2007, 83, 637-641.	1.3	5
67	DNA Photonics $\hat{a} \in$ "Probing Light-Induced Dynamics in DNA on the Femtosecond Timescale. Nanoscience and Technology, 2007, , 221-248.	1.5	1
68	Dynamics and Mechanism of Bridge-Dependent Charge Separation in Pyrenylureaâ^'Nitrobenzene Ï€-Stacked Protophanes. Journal of the American Chemical Society, 2006, 128, 4792-4801.	6.6	30
69	Crossover from Superexchange to Hopping as the Mechanism for Photoinduced Charge Transfer in DNA Hairpin Conjugates. Journal of the American Chemical Society, 2006, 128, 791-800.	6.6	164
70	Base pair motions control the rates and distance dependencies of reductive and oxidative DNA charge transfer. Proceedings of the National Academy of Sciences of the United States of America, 2006, 103, 10192-10195.	3.3	72
71	Determination of carbohydrates as their 3-aminophthalhydrazide derivatives by capillary zone electrophoresis with on-line chemiluminescence detection. Journal of Chromatography A, 2003, 992, 181-191.	1.8	28